# Large-Scale Synthesis of Colloidal $Fe_3O_4$ Nanoparticles Exhibiting High Heating Efficiency in Magnetic Hyperthermia

Yury V. Kolen'ko,*[,†] Manuel Bañobre-López,[†] Carlos Rodríguez-Abreu,[†] Enrique Carbó-Argibay,[†] Alexandra Sailsman,[‡] Yolanda Piñeiro-Redondo,[#] M. Fátima Cerqueira,[§] Dmitri Y. Petrovykh,[†] Kirill Kovnir,[⊥] Oleg I. Lebedev,[∥] and José Rivas[†]

[†]International Iberian Nanotechnology Laboratory, Braga 4715-330, Portugal
[‡]Department of Materials Science and Engineering, Massachusetts Institute of Technology, Cambridge MA 02139, USA
[#]Department of Applied Physics, University of Santiago de Compostela, Santiago de Compostela 15782, Spain
[§]Center of Physics, University of Minho, Braga 4710-057, Portugal
[⊥]Department of Chemistry, University of California at Davis, Davis CA 95616, USA
[∥]CRISMAT, UMR 6508, CNRS-ENSICAEN, Caen 14050, France
*yury.kolenko@inl.int

**This SI file includes a detailed description of characterization methods, Table S1, and Figures S1 to S5.**

## CHARACTERIZATION

### Transmission electron microscopy

Transmission electron microscopy (TEM), electron diffraction (ED) and high-resolution TEM (HRTEM) investigations were performed using Tecnai G2 30 UT and Titan ChemiSTEM transmission electron microscopes (FEI Company), operated at 300 kV and 200 kV and having 0.17 nm and 0.24 nm point resolutions, respectively. The samples for TEM were prepared by dropping ultrasonically dispersed NPs onto a holey carbon-coated Cu grid followed by the evaporation of the solvent. Image processing and geometrical phase analysis (GPA) were performed using Digital Micrograph software package (Gatan) and routines written for this software.

### Dynamic light scattering

The hydrodynamic diameter of the diluted colloids was measured at 298 K by means of dynamic light scattering (DLS) using SZ-100 nanoparticle analyser (Horiba). DLS measurements were performed on the NP dispersions prepared by dilution of colloidal stock solution followed by 5 min ultrasonication in an Elmasonic P bath (Elma). The experiments were carried out at a single scattering angle of 90° using a 532 nm diode-pumped solid-state laser. Particle size expressed as a Z-average value and polydispersity index were calculated using the method of cumulants. The data were averaged over six scans.

### Powder X-ray diffraction

Powder X-ray diffraction (XRD) data were collected on a X'Pert PRO diffractometer (PANalytical) set at 45 kV and 40 mA, and equipped with Cu $K\alpha$ radiation ($\lambda$=1.541874 Å). Data were collected using Bragg-Brentano geometry in the 15 to 80° $2\theta$ range with a scan speed of 0.006 °/s. Ge was used as an internal standard. The XRD patterns were matched to COD – Crystallography Open Database (Ref. 21a, MS) using HighScore software package (PANalytical). The unit cell parameters were calculated from least-squares refinements using the WinCSD software package (Ref. 21b, MS).

### Raman scattering

Raman scattering measurements were carried out on alpha300 R confocal Raman microscope (WITec) using a 532 nm Nd:YAG laser for excitation. The system was operated with an output laser power of around 100 μW to avoid sample degradation due to laser-induced heating. The laser beam was focused on the powder by a ×50 lens (Zeiss); and the spectra were collected with an 1800 groove/mm grating using 100 acquisitions with a 5 s acquisition time.

### X-ray photoelectron spectroscopy

The surface of NPs was probed by X-ray photoelectron spectroscopy (XPS) using an ESCALAB 250 Xi system (Thermo Scientific). The specimens of colloidal NPs were prepared for XPS analysis by drop casting the colloids onto Al foil (cleaned by UV-ozone treatment) with subsequent drying in vacuum at room temperature. The specimens of NPs in powder form were pressed into an In foil. In both cases care was taken to ensure that NPs were well attached to the supports: samples were lightly tapped and a magnet was passed over them to remove any loose material. ESCALAB 250 Xi is equipped with a monochoromated Al $K\alpha$ X-ray source, a hemispherical electron energy analyser, an automated sample stage, and a video camera for viewing the analysis position. Spatially uniform charge neutralization was provided by beams of low-energy (≤ 10 eV) electrons guided by a magnetic lens and by $Ar^+$ ions. The standard analysis spot of about 900×600 $\mu m^2$ was defined by the microfocused X-ray source. The data acquired under these conditions were checked for artefacts by control experiments with smaller spot sizes and with the mag-

netic lens turned off. The measurements were performed at room temperature in an ultra-high vacuum chamber with the base pressure < $5\times10^{-10}$ mbar; the charge neutralization device produced approximately $2\times10^{-7}$ mbar partial pressure of Ar during measurements.

The energy of the monochromated Al *Kα* X-ray source was measured to be within < 0.2 eV from 1486.6 eV. The binding energy (BE) scale of the analyser was calibrated to produce < 50 meV deviations of the three standard peaks from their standard values: 83.98 eV for Au $4f_{7/2}$, 368.26 eV for Ag $3d_{5/2}$, and 932.67 eV for Cu $2p_{3/2}$ (Ref. 22a, MS). The raw BE values in each dataset were corrected by ≤ 1.0 eV to place the aliphatic C 1s peak at 284.6 eV, i.e., the value that is commonly measured for organic monolayers on metal substrates (Ref. 22b, MS). This BE correction was verified by observing for each sample the same BE value of 530.0±0.1 eV for the O 1s component associated with iron oxide.

High-resolution elemental XPS data in C 1s, O 1s, and Fe 2p regions were acquired with the analyser pass energy set to 20 eV (corresponding to energy resolution of about 0.36 eV) and the step size set to 0.1 eV. Additional high-resolution scans were performed in regions corresponding to elements (including Al and In from supporting foils) expected to be present in samples or detected in wide survey scans. All the spectra were acquired in normal emission with an effective analyser collection angle of about 30°.

Avantage software package (Thermo Fisher Scientific) was used to quantify the elemental spectra (including the standard "atomic %" elemental compositions) based on calibrated analyser transmission functions, Scofield sensitivity factors (Ref. 22c, MS), and effective attenuation lengths for photoelectrons from the standard TPP-2M formalism (Ref. 22d, MS).

## Quantification of the O/Fe Ratio

To estimate the surface oxide composition from XPS data, we use the areas of O 1s component that correspond to iron oxide (O–Fe in Figure 7) and of Fe 3p peak (high-resolution data not shown, peak indicated in Figure S3) with the standard "atomic %" normalization. Fe 3p rather than Fe 2p peak area is used because the intensity of the former can be estimated with lower uncertainty. For **PAA-CP** and **PAA-HT**, the O/Fe ratio is approximately 2.4±0.1, which is above the stoichiometry of any iron oxide. The apparent oxide O/Fe ratio is <1 for the **OL-HT** sample, suggesting an overall oxide composition with roughly 1:1 stoichiometry. The O/Fe ratio lower than that for the PAA-coated $Fe_3O_4$, however, is likely the result of the dominant contribution from a much thicker organic overlayer and the corresponding attenuation of the direct signal from the organic–NP interface (both effects are clearly evident in Figure S3), in agreement with the interpretation of the XPS data for the organic coatings (Figure 7).

## Thermogravimetry – differential scanning calorimetry – mass spectrometry

The thermal behaviour of the products was studied by means of thermogravimetry and differential scanning calorimetry coupled to online mass spectrometry (TGA-DSC-MS) using TGA/DSC 1 STAR$^e$ system (Mettler-Toledo) fitted with OmniStar GSD320 gas analysis system (Pfeiffer Vacuum). The samples were heated from 303 to 1273 K at 10 K/min under a continuous Ar flow of 50 mL/min. The concentration of NPs in the dispersions was also determined using TGA-DSC. The colloids were heated from 298 to 973 K at 5 K/min under a continuous Ar flow of 50 mL/min. The concentration data were averaged over three experiments.

## Weight loss analysis

The TGA profiles exhibit stepwise weight loss curves; the total weight losses between 303 and 1273 K in argon are recorded to be approximately 6.2, 9.3, and 15.0% for the **PAA-CP**, **PAA-HT** and **OL-HT**, respectively.

As an example, we show results for **OL-HT** (Figure S4). We observe that the total weight loss of the samples consists of three main contributions. The first step (up to about 600 K) corresponds to the endothermic desorption of physically adsorbed water, as confirmed by $m/z$ = 18 peak of $H_2O$ in the MS ion curve. In the second step, the exothermic decomposition step of oleate coating begins from approximately 600 K and is largely completed at around 700 K. The intense peak at $m/z$ = 2 in the MS ion curve demonstrates that the oleate coatings are mainly decomposed via dehydrogenation with intensive $H_2$ release at this step (in addition to $CO_2$ release). Finally, the third step (700−1000 K) is associated with further degradation of the resultant carbonic residues, as manifested by the intense $CO_2$ peak at $m/z$ = 44 in the MS ion curve (in addition to $H_2$ release), proving the presence of the carboxylic group containing oleate in the sample. Notable, at the temperatures above 1000 K, we observed a slight increase in mass of the test sample with an interruption at around 1150 K. During this interruption, it appears that the surface of $Fe_3O_4$ undergoes partial reduction through the reaction with $H_2$ and C, the simultaneously recorded MS ion curves show $H_2$ and mainly $CO_2$ evolving from the sample. This reduction yields an admixture of wüstite (FeO) phase in the sample after TGA-DSC-MS experiment, as confirmed by the XRD analysis.

## Colloidal stability

For the temperature dependent colloidal stability, 0.01% dispersions of the NPs in solvent were made. Target temperatures of the dispersions ranged from 298 to 363 K with a step of 10 K, and once reached were maintained for a period of 5 min. The colloidal stability in water of PAA-coated NPs as a function of ionic strength was tested by preparing 0.01% dispersions of the NPs in NaCl (99.5%, Sigma-Aldrich) solutions of varying molarity.

## Magnetic measurements

Magnetic measurements were carried out on powder samples by using a superconducting quantum interference device (SQUID) magnetometer SQUID-VSM and Vibrating Sample Magnetometer (VSM) EV9 manufactured by Quantum Design and Lot-Oriel, respectively. For measurements, the particles were precipitated from the colloidal stock solution by adding ethanol, centrifuged, dried overnight in vacuum at room temperature, ground in agate mortar and pestle, and finally placed in gelatin capsules for measurements. Zero-field-cooled (ZFC) and field-cooled (FC) magnetization curves were obtained over a temperature range of 2−300 K. Hysteresis loops were obtained at 300 K applying a magnetic field up to ±20,000 Oe.

## Magnetic hyperthermia measurements

Magnetic hyperthermia data were acquired on a DM 100 system (nB nanoScale Biomagnetics) using oscillating magnetic fields of frequencies up to 300 kHz and intensities up to 300 Oe. Measurements were carried out on 1-mL samples of NP dispersions in water (15 g/L), which were introduced into a glass vial and placed at the mid-point of a water-cooled copper coil. Temperature versus time plots were recorded by using an optical-fiber-based thermometer.

## TABLES

**Table S1. Summary of Lorentzian fit of Raman data for the synthesized colloids.**

| Sample | $A_{1g}$ ($Fe_3O_4$) $\omega_o$[a]/FWHM[b] ($cm^{-1}$) | $A_{1g}$ ($\gamma$-$Fe_2O_3$) $\omega_o$/FWHM ($cm^{-1}$) | Intensity ratio I(720)/I(670) |
|---|---|---|---|
| **PAA-CP** | 670/60 | 720/50 | 0.18 |
| **PAA-HT** | 670/60 | 720/50 | 0.33 |
| **OL-HT** | 670/85 | 720/50 | 0.71 |

[a] Peak position. [b] Full width at half maximum.

## FIGURES

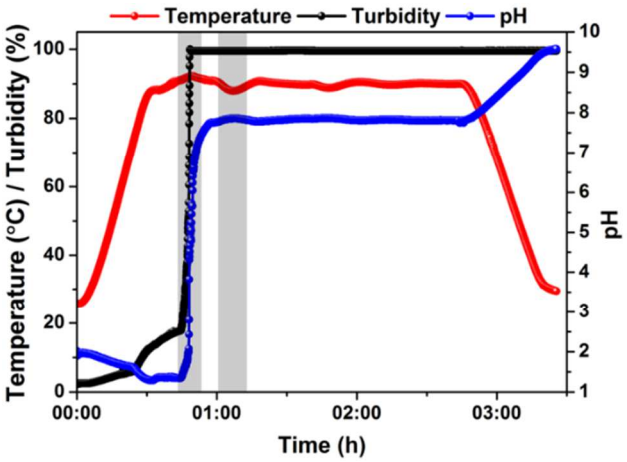


**Figure S1.** Time log of an automated reactor synthesis (363 K, 1 h) showing temperature, turbidity, and pH. Left region shaded in grey indicates addition of aqueous ammonia solution, while the right one marks addition of poly(acrylic acid sodium salt) solution.

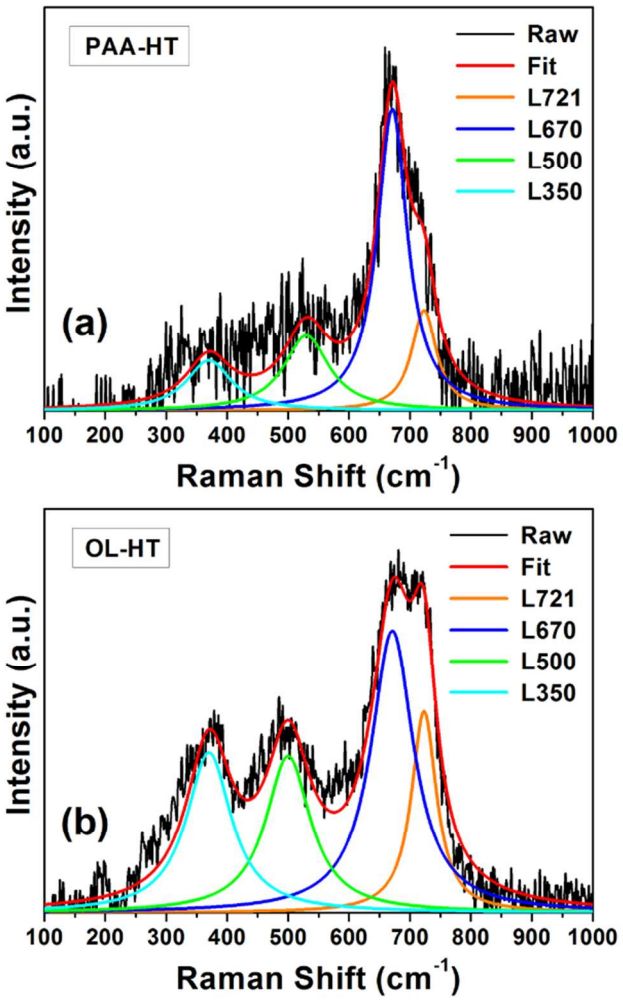


**Figure S2.** Lorentzian fit (red line) of Raman data (black line) for selected PAA-coated (a) and OL-coated (b) $Fe_3O_4$ NPs synthesized by hydrothermal method.

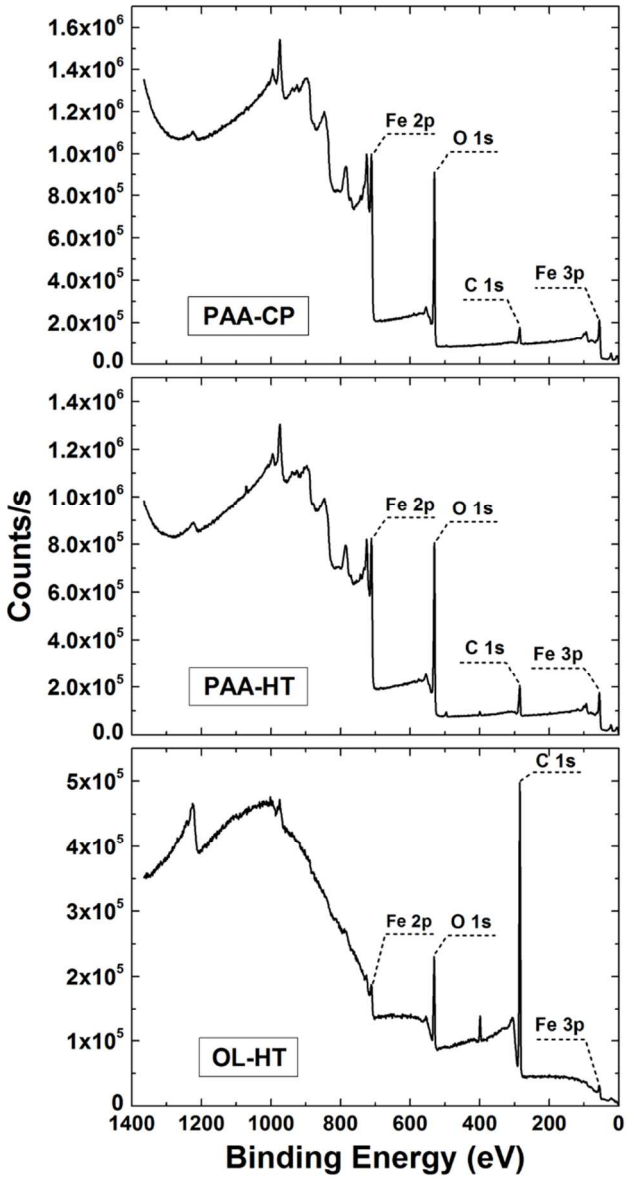


**Figure S3.** XPS survey data for the synthesized colloids. Fe 2p, C 1s, O 1s, and Fe 3p peaks discussed in the main text are indicated.

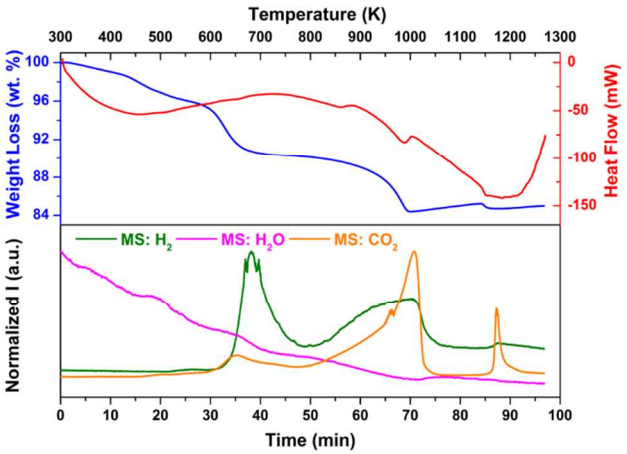


**Figure S4.** Thermal degradation of the organic coating in a selected **OL-HT** sample. Thermal decomposition of oleate coating under Ar atmosphere, as followed by mass spectrometry, is accompanied by the formation of hydrogen ($m/z$ = 2), water ($m/z$ = 18), and carbon dioxide ($m/z$ = 44).

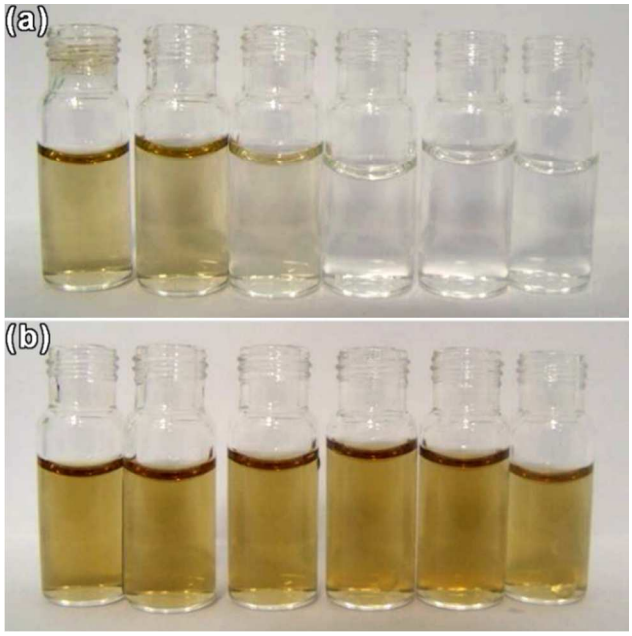


**Figure S5.** Colloidal stability as a function of ionic strength for PAA-coated $Fe_3O_4$ NPs synthesized by controlled co-precipitation (a) and by hydrothermal method (b). Molar concentration of NaCl from left to right is 0.01 M, 0.02 M, 0.04 M, 0.06 M, 0.08 M, and 0.1 M.